

Langer Gerald (Orcid ID: 0000-0002-7211-4889)
Greaves Mervyn (Orcid ID: 0000-0001-8014-8627)
Misra Sambuddha (Orcid ID: 0000-0002-8825-451X)

Title

Li partitioning into coccoliths of *Emiliana huxleyi*: evaluating the general role of “vital effects” in explaining element partitioning in biogenic carbonates

Authors and affiliations:

Gerald Langer¹, Aleksey Sadekov², Mervyn Greaves³, Gernot Nehrke⁴, Ian Probert⁵, Sambuddha Misra⁶, Silke Thoms⁴

1 The Marine Biological Association of the United Kingdom, The Laboratory, Citadel Hill, Plymouth, Devon, PL1 2PB, UK

2 ARC Centre of Excellence for Coral Reef Studies, Ocean Graduate School, The University of Western Australia, 35 Stirling Highway, Crawley WA 6009

3 The Godwin Laboratory for Palaeoclimate Research, Department of Earth Sciences, University of Cambridge, Downing St., Cambridge. CB2 3EQ. UK

4 Alfred Wegener Institute, Helmholtz Centre for Polar and Marine Research, Bremerhaven, Germany

5 Sorbonne Université / Centre National de la Recherche Scientifique, Roscoff Culture Collection, FR2424, Station Biologique de Roscoff, 29682 Roscoff, France

6 Centre for Earth Sciences, Indian Institute of Science, Bangalore-560012, India

Corresponding author: Gerald Langer (gerlan@MBA.ac.uk)

Key Points:

- 1) The Li partitioning pattern of *E. huxleyi* resembles that of *A. lessonii* and inorganic calcite
- 2) Li partitioning in *E. huxleyi* is dominated by a coupled transmembrane transport of Li and Ca
- 3) The vital effect is ubiquitous in calcifying organisms, even if it appears to be absent

This article has been accepted for publication and undergone full peer review but has not been through the copyediting, typesetting, pagination and proofreading process which may lead to differences between this version and the Version of Record. Please cite this article as doi: 10.1029/2020GC009129

Abstract

Emiliana huxleyi cells were grown in artificial seawater of different Li and Ca concentrations and coccolith Li/Ca ratios determined. Coccolith Li/Ca ratios were positively correlated to seawater Li/Ca ratios only if the seawater Li concentration was changed, not if the seawater Ca concentration was changed. This Li partitioning pattern of *E. huxleyi* was previously also observed in the benthic foraminifer *Amphistegina lessonii* and inorganically precipitated calcite. We argue that Li partitioning in both *E. huxleyi* and *A. lessonii* is dominated by a coupled transmembrane transport of Li and Ca from seawater to the site of calcification. We present a refined version of a recently proposed transmembrane transport model for Li and Ca. The model assumes that Li and Ca enter the cell via Ca channels, the Li flux being dependent on the Ca flux. While the original model features a linear function to describe the experimental data, our refined version uses a power function, changing the stoichiometry of Li and Ca. The version presented here accurately predicts the observed dependence of D_{Li} on seawater Li/Ca ratios. Our data demonstrate that minor element partitioning in calcifying organisms is partly mediated by biological processes even if the partitioning behaviour of the calcifying organism is indistinguishable from that of inorganically precipitated calcium carbonate.

Plain Language Summary

Marine shell-forming organisms such as the minute, but abundant, coccolithophores (single celled phytoplankton) and foraminifera (single celled zooplankton) are not only ecologically important, but also contribute significantly to the global carbonate sink. Minor elements (e.g. Sr and Li) trapped in biogenic carbonate sediments provide a window into past environmental conditions such as temperature, which is relevant for climate change. An understanding of elemental incorporation processes is required in order to correctly translate these minor element signatures into past environmental data. Here we conducted culture experiments with the coccolithophore *Emiliana huxleyi* to determine its Li incorporation behaviour. We compare our results with previously published data on the foraminifer *Amphistegina lessonii* and data on synthetic calcite. The Li incorporation behaviour of biogenic calcites is surprisingly similar to that of synthetic calcite. This is usually taken to mean that Li incorporation into shells should proceed inorganically. By contrast, we conclude that minor element incorporation processes in marine shell-forming organisms always include biological processes. This is relevant to past climate reconstructions because it excludes any interpretation of minor element signatures in fossil shells based on inorganic processes only.

Introduction

Minor element (Me) incorporation into marine biogenic carbonates has been widely used to reconstruct environmental parameters such as temperature and seawater chemistry (Elderfield et al. 2000, Lea 2014). For instance, seawater Sr/Ca ratios and Li/Ca ratios were reconstructed from foraminiferal Sr/Ca ratios and Li/Ca ratios respectively (Delaney and Boyle 1986, Lear et al. 2003, Hathorne and James 2006). These reconstructions assume a positive relationship between foraminiferal Me/Ca ratios and seawater Me/Ca ratios. Culture studies have shown that this assumption indeed holds true for Sr, not only in foraminifera but also in coccolithophores (Langer et al. 2006, Langer et al. 2016, Hermoso et al. 2017, Mejia et al. 2018, Müller et al. 2018). However, while Mg partitioning into foraminiferal calcite shows a behaviour similar to that of Sr partitioning (Mewes et al. 2014, Mewes et al. 2015a), foraminiferal Li/Ca does not depend on seawater Li/Ca, but on seawater Li concentration (Langer et al. 2015). At first glance this difference between divalent cation Sr (Mg) and the alkali metal ion Li, could be explained in terms of inorganic precipitation processes. In contrast to divalent ions, alkali metal ions do not compete with Ca for a position in the calcite lattice (Lorens, 1981; Ishikawa and Ichikuni, 1984; Busenberg and Plummer, 1985; Okumura and Kitano, 1986; Marriott et al., 2004a). However, any inorganic precipitation based explanation of the minor element partitioning behaviour of calcifying organisms has to face the persistent issue of the “vital effect”, first mentioned by Urey et al. (1951): “we may ask whether there is a vital effect?”.

The vital effect is usually discussed whenever there is a discrepancy between the minor element partitioning behaviour of a calcifying organism and inorganic precipitation, but often ignored when there is no discrepancy. In the latter case it is usually implied that minor element partitioning is driven by inorganic precipitation alone, but this might be mistaken. The U partitioning into foraminiferal calcite, for example, was first explained in terms of inorganic precipitation alone (Russell et al. 2004), but later inorganic precipitation combined with cellular U transport was suggested as an alternative explanation (Keul et al. 2013). This is where conceptual biomineralization models enter the debate. These models have been developed for different calcifiers based on a number of observations in various fields of research such as physiology, biochemistry, anatomy, ultrastructure, and elemental fractionation itself (Simkiss and Wilbur 1989, Vidavsky et al. 2016, Bentov et al. 2009, Gagnon et al. 2012, Erez 2003, Erez and Braun 2007, Tambutté et al. 2012, Mass et al. 2017, Nehrke et al. 2013, Langer et al. 2006). The common feature of all these models is that they include biological processes in the overall partitioning mechanism of minor elements. They

raise the question of the “invisible vital effect”, in other words mimicry of inorganic partitioning behaviour (Taubner et al., 2012; Keul et al., 2013; Gussone et al., 2016). Li partitioning into foraminiferal calcite is a prime example. Although the pattern of Li partitioning into *Amphistegina lessonii* is explicable in terms of inorganic precipitation, an explanation based on transmembrane transport of ions was proposed (Langer et al. 2015). This explanation presupposes that foraminifera actually use transmembrane transport in order to deliver Ca ions to the site of calcification. However, even though several studies are in favour of this view (Glas et al. 2012, Nehrke et al. 2013, Keul et al. 2013, Mewes et al. 2015a, Langer et al. 2016), there are still numerous studies proposing endocytosis of seawater as a mechanism by which Ca is transported to the site of calcification (Erez 2003, Bentov et al. 2009, Evans et al. 2018). Coccolithophores, by contrast, solely use transmembrane transport to deliver Ca and other ions to the coccolith vesicle (Taylor et al. 2017). Here we ask the following question: Does the Li partitioning behaviour of *Emiliana huxleyi* resemble that of *A. lessonii*? If the Li partitioning behaviour of *E. huxleyi* was fundamentally different (dependence of coccolith Li/Ca on seawater Li/Ca) from that of *A. lessonii*, it would be highly likely that Li partitioning in this foraminifer is not driven by transmembrane transport. If the Li partitioning behaviour of *E. huxleyi* was similar to that of *A. lessonii* this would show that a transmembrane based partitioning mechanism could produce the Li partitioning pattern we see in *A. lessonii*.

Since there are no published data on Li partitioning in coccolithophores, we conducted an experiment with *E. huxleyi*, similar in setup to the one performed on *A. lessonii* (Langer et al. 2015).

Material and Methods

Culture experiments:

Clonal cultures of *Emiliana huxleyi* (strain RCC3652) were obtained from the Roscoff Culture Collection (<http://roscoff-culture-collection.org/>) and grown in triplicate in sterile filtered (0.2 µm pore-size cellulose-acetate filters) artificial seawater (for general composition of major ions except Ca see Langer et al. 2006, Langer et al. 2009, for particular changes to this composition with respect to Ca and Li see Table 1; all salts reagent grade, obtained from Merck) enriched with 100 µmol L⁻¹ nitrate, 6.25 µmol L⁻¹ phosphate, and trace metals and vitamins according to f/2 (Guillard and Ryther, 1962). The incident photon flux density was 250 µmol/m²*s and a 16/8 h light/dark cycle was applied. Experiments were carried out at 20°C. Two separate experiments were conducted. In one experiment the Li concentration of

the artificial seawater was varied, and in the other experiment the Ca concentration of the artificial seawater was varied. For details on Li and Ca concentrations see Table 1. The pH of the artificial seawater was adjusted to 8.2 (NBS scale) by sodium hydroxide (0.1 M) addition. Seawater pH was determined potentiometrically using a glass electrode/reference electrode cell (Schott Instruments, Mainz, Germany), which included a temperature sensor and was two-point calibrated with NBS buffers prior to every set of measurements. Average repeatability was ± 0.02 pH units ($n = 30$). Salinity of the artificial seawater was determined by means of a conductivity meter (WTW Multi 340i) combined with a TetraCon 325 sensor. Cells were grown in dilute batch ensuring a quasi-constant carbonate chemistry over the course of the experiment (Langer et al. 2011). Cell densities were determined by means of flow cytometry. Cultures were harvested by filtering onto Omnipore polycarbonate membrane filters (0.8 μm pore-size) using a vacuum pump. The filters were dried at 50 °C for 24 hours prior to storage at room temperature.

Sample preparation and determination of Me/Ca ratios:

Approximately 15-20 mg of the sample were subsampled from each filter by folding the filter with plastic tweezers and collecting flakes of material in 5 ml acid pre-cleaned centrifuge tubes. To remove organic matter and residual seawater 4ml of 10% hydrogen peroxide were added to each sample tube and heated to $\sim 60^\circ\text{C}$ and ultrasonicated for 10 mins. The sample was subsequently centrifuged to pellet the solid fraction and remove/exchange the residual solution. This procedure was repeated 4 times and followed by 4 rinses in water with ultrasonication and centrifugation in a similar way to the peroxide treatment. Type 1 (18.2 M Ω) purified water was used for all rinses. The rinses most likely only dissolved a negligible percentage of the sample, which does not affect the Li/Ca ratio (Yu et al. 2007).

We also left the samples in water for 12h as a final 5th rinse to further remove potential seawater contamination. Samples were left to dry after the final centrifugation and removal of the supernatant.

*Analyses of cultured *Emiliana huxleyi*:*

Subsamples of the prepared *Emiliana huxleyi* were transferred to 0.5 ml microcentrifuge tubes and rinsed a further time by adding 500 μl water, sonicating to mix the suspension and centrifuging. The supernatant water was removed and the samples dissolved in 500 μl 0.1M HNO_3 . The solution was centrifuged and 450 μl supernatant saved for analysis. A 25 μl aliquot was diluted 10 fold for Ca determination by ICP-OES. The Ca concentrations confirmed that sample sizes ranging from 1.7 to 7.2 mg CaCO_3 had been dissolved. Aliquots

of the remaining solution were diluted to constant Ca concentration for the determination of Li/Ca and Sr/Ca ratios. Sr/Ca was determined by ICP-OES using the method of de Villiers et al. (2002). Analytical precision for Sr/Ca is better than 0.3 % (r.s.d), determined by replicate runs of a consistency standard containing 1.67 mmol/mol Sr/Ca.

Li/Ca ratios of *Emiliania huxleyi* were determined on a Thermo ElementXR sector field ICP-MS at the Department of Earth Sciences, University of Cambridge following the method detailed in Misra et al (2014). Long term analytical precision for Li/Ca of 3.6% (1 σ r.s.d.) has been established over a four year period, based on replicate measurements of an in-house foraminifera standard (CAM-Uvig-2) containing 13.5 μ mol/mol Li/Ca.

Analyses of culture media:

The culture media were analysed in the same manner as previously for *A. lessonii* culture experiments (Langer et al, 2015). Briefly, Li/Ca and Sr/Ca ratios were determined by ICP-OES after dilution of the culture media to a constant sodium concentration of 110 ppm. Samples were run on a Varian Vista Axial ICP-OES using the 315.887 nm Ca, 421.552 nm Sr and the 670.783 nm Li emission lines. Calibration standards were prepared from IAPSO standard seawater to closely match the concentration matrix of the media solutions, spiked with Ca, Li and Sr (also Mg) to cover the concentration ranges in the experiments. Precision better than 0.5 % (r.s.d) was achieved for both Li/Ca and Sr/Ca, determined by replicate runs of a consistency standard containing 14.5 mmol/mol Li/Ca, and 30.6 mmol/mol Sr/Ca. seawater Li/Ca is changed by altering Li concentration, coccolith Li/Ca is positively correlated to seawater Li/Ca (Fig 1). If, on the other hand, seawater Li/Ca is changed by adjusting the Ca concentration, coccolith Li/Ca is negatively correlated to seawater Li/Ca (Fig 2). This pattern is in stark contrast to the behaviour of Sr, i.e. changing the seawater Sr/Ca by changing seawater Ca concentration yields a positive correlation between coccolith Sr/Ca and seawater Sr/Ca (Fig 3). Our Sr data tally well with published data on both *E. huxleyi* and *Amphistegina lessonii* in the sense that calcite Sr/Ca depends on seawater Sr/Ca, as opposed to seawater Sr concentration (Langer et al. 2006, Langer et al. 2016). As a general caveat we point out that the number of data points used in our and similar studies (references see above, also Introduction) is not sufficient to run statistical significance tests. Nevertheless, the relationships described here and elsewhere are sufficiently unambiguous to justify the conclusions drawn. At any rate, it would be desirable to conduct additional studies in the future including more data points and statistical tests.

However, coccolith Li/Ca only increases if seawater Li concentration is increased, not if seawater Ca concentration is decreased. This pattern was also reported for *A. lessonii* (Langer et al. 2015). Hence the Li partitioning pattern is the same in inorganically precipitated calcite (Okumura and Kitano 1986, Marriott et al. 2004a), *A. lessonii* (Langer et al. 2015), and *E. huxleyi* (this study). It is generally accepted that coccolithophores employ transmembrane transport to deliver Ca ions to the coccolith vesicle (Taylor et al. 2017), and interpretations of minor element and isotope partitioning into coccoliths have been based on conceptual biomineralization models featuring transmembrane transport of Ca and the minor element in question (Langer et al. 2006, Gussone et al. 2006, Langer et al. 2009, Stoll et al. 2012). We therefore propose that the similarity in partitioning pattern between inorganically precipitated calcite and *E. huxleyi* coccoliths is not based on a similarity in partitioning mechanism, but represents a case of mimicry, i.e. transmembrane transport of Li and Ca in *E. huxleyi* creates a partitioning pattern that looks like that of inorganically precipitated calcite. Consequently, the Li partitioning pattern of *A. lessonii* could also represent a case of inorganic mimicry (Langer et al. 2015). To analyse the Li partitioning pattern in more detail we adopt the model of a coupled transmembrane transport of Li and Ca proposed by Langer et al. (2015), which is based on the idea that Li can enter the cell via Ca channels. In Langer et al. (2015), the authors used a linear function to describe their experimental data. While this is possible also for *E. huxleyi*, a more in depth qualitative analysis of the data, both *E. huxleyi* and *A. lessonii*, leads us to conclude that a power function serves the purpose better. The usage of a power function does not change the underlying idea of the model, but merely the stoichiometry of the Li and Ca transport. According to the model the Li flux (F_{Li}) is:

$$F_{Li} = k[Li]_{SW}^x [Ca]_{SW}^y \quad (1)$$

As suggested in Langer et al. (2015), the Ca flux is probably not significantly affected by the Li ion due to the small size of the latter, and is therefore described as:

$$F_{Ca} = l[Ca]_{SW} \quad (2)$$

which is a valid description for the channels as well as for a non-saturated active transport process. Then, the Li/Ca of the precipitated calcite is given by the ratio of the ion fluxes:

$$\left(\frac{Li}{Ca}\right)_{CC} = \frac{F_{Li}}{F_{Ca}} = \frac{k}{l} [Ca]_{SW}^{y-1} [Li]_{SW}^x = \frac{k}{l} [Ca]^{y-1+x} R_{SW}^x \quad (3)$$

where R_{SW} is the seawater Li/Ca. To illustrate the advantage of a power function we re-plotted the *A. lessonii* data against R_{SW} and applied equation (3), as we did for *E. huxleyi* (Fig 1). Equation (3) indicates that the calcite Li/Ca is correlated to R_{SW} with a positive power ($x = 0.829$) only if the Li concentration of seawater is changed. From the last term in equation

(3) follows the observed power function describing the positive correlation between the calcite Li/Ca and the seawater Li/Ca at constant Ca concentration:

$$\left(\frac{Li}{Ca}\right)_{CC} = \frac{k}{l} [Ca]_{SW}^{y-1+x} R_{SW}^x = const_1 R_{SW}^x \quad (4)$$

However, if the Ca concentration of seawater is changed, while keeping Li concentration constant, the calcite Li/Ca is negatively correlated to R_{SW} , which is indicated by a negative power ($1-y = -0.2$) in equation (5):

$$\left(\frac{Li}{Ca}\right)_{CC} = \frac{k}{l} [Li]_{SW}^{x+y-1} R_{SW}^{1-y} = const_2 R_{SW}^{1-y} \quad (5)$$

The change in the Li partitioning coefficient D_{Li} with changing seawater Li/Ca for both experimental setups can immediately be derived by using equations (4) and (5), respectively. If the Li concentration of seawater is changed it follows from equation (4) a power function for the relationship between D_{Li} and R_{SW} :

$$D_{Li} = \frac{1}{[Li]_{SW}} \left(\frac{Li}{Ca}\right)_{CC} = \frac{const_1}{[Ca]_{SW}} R_{SW}^{x-1} = const_3 R_{SW}^{x-1} \quad (6)$$

For the case of changing Ca concentration, the power function for D_{Li} is given by:

$$D_{Li} = \frac{1}{[Li]_{SW}} \left(\frac{Li}{Ca}\right)_{CC} = \frac{const_2}{[Li]_{SW}} R_{SW}^{1-y} = const_4 R_{SW}^{1-y} \quad (7)$$

Here, two features are particularly interesting. Firstly, the model curves describe not only the correlation between calcite Li/Ca and seawater Li/Ca, but the predicted change in D_{Li} with changing seawater Li/Ca fits the experimental data. Secondly, the relationships in *A. lessonii* and *E. huxleyi* are remarkably similar (Figs 1 and 4). This similarity points to a similar underlying mechanism. We emphasise that this similarity does not prove a common Li partitioning mechanism in *A. lessonii* and *E. huxleyi*, but it renders a common mechanism possible, and even likely. We propose that this common mechanism is dominated by coupled transmembrane transport of Li and Ca, as suggested by Langer et al. (2015).

However, despite the striking similarity in Li partitioning patterns of *A. lessonii* and *E. huxleyi*, there are also differences. If the seawater Li/Ca is changed by altering seawater Ca concentration, the *A. lessonii* Li/Ca ratio remains constant, whereas the *E. huxleyi* Li/Ca ratio increases at low seawater Li/Ca (Langer et al. 2015, and Fig 2). The reason for this could be the bigger range in seawater Li/Ca in the *E. huxleyi* experiment. Regardless of the reason for this difference, the important observation here is that in both *A. lessonii* and *E. huxleyi* there is no positive correlation between calcite Li/Ca and seawater Li/Ca if the latter is changed by changing seawater Ca concentration, in contrast to divalent cations such as Sr and Mg (this study, Langer et al. 2006, Mewes et al. 2014, Mewes et al. 2015a, Mewes et al. 2015b,

Langer et al. 2016). This underlines that in both *A. lessonii* and *E. huxleyi* the alkali metal Li behaves differently from the divalent cations Sr and Mg.

The other difference between the Li partitioning behaviour of *A. lessonii* and *E. huxleyi* concerns the partitioning coefficient D_{Li} . The partitioning coefficient of a minor element (Me) is usually calculated according to $D_{Me} = (Me/Ca)_{cc}/(Me/Ca)_{sw}$ (e.g. Lorens et al. 1981). While this definition works well for divalent cations, the D_{Me} of alkali cations such as Li should be calculated according to $D_{Me} = (Me/Ca)_{cc}/[Me]_{sw}$ (Busenberg and Plummer 1985; Okumura and Kitano 1986, Langer et al. 2015). However, even some recent studies still use the former definition of the partitioning coefficient for alkali metal ions (Evans et al. 2018, Fuger et al. 2019). In order to put our *E. huxleyi* D_{Li} in the context of literature data we therefore use both definitions of D_{Li} . From Fig 5 the following conclusions may be drawn: 1) *A. lessonii* D_{Li} is higher than *E. huxleyi* D_{Li} , 2) different foraminifera have similar D_{Li} , 3) *E. huxleyi* D_{Li} falls within the range of values for inorganic calcite, 4) *A. lessonii* D_{Li} is higher than the one of inorganic calcite.

Please note that values for $D_{Li} = (Li/Ca)_{cc}/(Li/Ca)_{sw}$ are potentially misleading, even when only used as relative values. This is due to the variable Ca concentration used in different experiments. However, only conclusion 2 (see above) relies on this potentially misleading definition of D_{Li} alone. We are therefore cautious with respect to conclusion 2 but confident with respect to conclusions 1, 3, and 4. Taken together with the other data discussed above, this comparison of different D_{Li} suggests that *E. huxleyi* displays a complete mimicry of inorganic Li partitioning behaviour whereas *A. lessonii* does so only partially, i.e. the *A. lessonii* D_{Li} differs from the inorganic one. The question of whether the latter difference is indicative of a fundamental difference in partitioning mechanism between *A. lessonii* and *E. huxleyi*, or is merely indicative of different membrane characteristics (e.g. calcium channels, White 2000), cannot be answered with certainty. However, the absolute Li fractionation of e.g. Ca channels in the plasmamembrane of foraminifera might well be different from that of coccolithophores. This difference would be sufficient to explain the difference in D_{Li} between *A. lessonii* and *E. huxleyi*, without the need to invoke a fundamental difference in fractionation mechanism such as different cellular pathways for Li and Ca, e.g. vesicle transport in foraminifera and transmembrane transport in coccolithophores. Taken together with other support for Ca and minor element transmembrane transport in foraminifera (Glas et al. 2012, Nehrke et al. 2013, Keul et al. 2013, Mewes et al. 2015a, Langer et al. 2016), we conclude that there is no fundamental difference in Li partitioning mechanism between *A. lessonii* and *E. huxleyi*. The most plausible interpretation is that both species feature a

coupled transmembrane transport of Li and Ca, accounting for the Li partitioning behaviour described above. However, transmembrane transport of Li and Ca in *A. lessonii* does not exclude additional fractionation steps such as a precursor phase (Jacob et al. 2017), which would introduce a constant offset of the curves but not change their shapes. The need to combine physiological and mineralogical fractionation steps in a description of the minor element incorporation behaviour of *A. lessonii* was previously highlighted for the divalent cation Mg (Mewes et al. 2015b, Langer et al. 2016). The discovery of a metastable precursor phase for shell calcite in foraminifera (Jacob et al. 2017) could perhaps explain why D_{Li} in *A. lessonii* is different from that of *E. huxleyi*, because there is currently no evidence for a precursor phase in coccolithophores.

Conclusion

This study indicates that the issue of the vital effect is omnipresent in calcifying organisms, even when the partitioning behaviour of the organism in question is indistinguishable from that of inorganically precipitated calcium carbonate. We do not conclude that every calcifying organism actually does show a vital effect, but we conclude that a vital effect cannot be excluded in any organism based on minor element partitioning data. The latter conclusion is based on the observation that *E. huxleyi* shows a complete mimicry of inorganic partitioning behaviour, although its calcification mechanism is substantially different from inorganic precipitation. While these conclusions can be confidently drawn from our data, the number of data points puts limits on statistical significance tests which would make the exact relationships more robust. Future studies should therefore include more data points so that statistical significance tests can be performed.

Acknowledgments, Samples, and Data

All data supporting the conclusions can be obtained from the MBA data repository: DOI <https://doi.org/10.17031/ykdq-wy51>. This work was supported by the Natural Environment Research Council (NE/N011708/1).

References

- Bentov, Shmuel, Colin Brownlee, Jonathan Erez (2009) The role of seawater endocytosis in the biomineralization process in calcareous foraminifera. *Proceedings of the National Academy of Sciences of the United States of America* vol. 106, 21500–21504
- Busenberg, E., and L. N. Plummer (1985) Kinetic and thermodynamic factors controlling the distribution of SO_3^{2-} and Na^+ in calcites and selected aragonites, *Geochim. Cosmochim. Acta*, 49, 713–725
- Delaney, M. L., and E. A. Boyle (1986), Lithium in foraminiferal shells: Implications for high-temperature hydrothermal circulation fluxes and oceanic crustal generation rates, *Earth Planet. Sci. Lett.*, 80, 91–105
- de Villiers, S., Greaves, M., Elderfield, H., 2002. An intensity ratio calibration method for the accurate determination of Mg/Ca and Sr/Ca of marine carbonates by ICP-AES. *Geochemistry, Geophysics, Geosystems* 3.
- Elderfield, H., M. Cooper, and G. Ganssen (2000), Sr/Ca in multiple species of planktonic foraminifera: Implications for reconstructions of seawater Sr/Ca, *Geochem. Geophys. Geosyst.*, 1, 1017, doi:10.1029/1999GC000031
- Erez J (2003) The source of ions for biomineralization in foraminifera and their implications for paleoceanographic proxies. *Rev Mineral Geochem* 54:115–149
- Erez J, Braun A (2007) Calcification in hermatypic corals is based on direct seawater supply to the biomineralization site. *Geochim Cosmochim Acta* 71(15 Suppl 1):A260
- Evans, D., Müller, W., Erez, J. (2018) Assessing foraminifera biomineralisation models through trace element data of cultures under variable seawater chemistry, *Geochimica et Cosmochimica Acta* 236, 198-217
- Füger, A., F. Konrad, A. Leis, M. Dietzel, V. Mavromatis (2019) Effect of growth rate and pH on lithium incorporation in calcite. *Geochimica et Cosmochimica Acta* 248, 14-24

Gagnon, Alexander C., Jess F. Adkins, Jonathan Erez (2012) Seawater transport during coral biomineralization, In *Earth and Planetary Science Letters*, Volumes 329–330, 150-161

Glas, M.S., Langer, G., Keul, N. (2012) Calcification acidifies the microenvironment of a benthic foraminifer (*Ammonia* sp.). *J. Exp. Mar. Bio. Ecol.* 424-425, 53–58.
doi:10.1016/j.jembe.2012.05.006

Guillard, R.R.L., Ryther, J.H. (1962) Studies of marine planktonic diatoms, I, *Cyclotella nanna* (Hustedt) and *Detonula convolvacea* (Cleve). *Can. J. Microbiol.* 8, 229–239

Gussone, N., Filipsson, H., Kuhnert, H. (2016) Mg/Ca, Sr/Ca and Ca isotope ratios in benthonic foraminifers related to test structure, mineralogy and environmental controls. *Geochim. Cosmochim. Acta* 173, 142–159

Gussone, N., Langer, G., Thoms, S., Nehrke, G., Eisenhauer, A., Riebesell, U., Wefer, G. (2006): Cellular calcium pathways and isotope fractionation in *Emiliania huxleyi*, *Geology* 34, 625-628. doi: 10.1130/G22733.1

Hathorne, E. C., and R. H. James (2006) Temporal record of lithium in seawater: A tracer for silicate weathering?, *Earth Planet. Sci. Lett.*, 246, 393–406

Hermoso M, Lefeuvre B, Minoletti F, de Rafélis M (2017) Extreme strontium concentrations reveal specific biomineralization pathways in certain coccolithophores with implications for the Sr/Ca paleoproductivity proxy. *PLoS ONE* 12(10): e0185655.
<https://doi.org/10.1371/journal.pone.0185655>

Ishikawa, M., and M. Ichikuni (1984), Uptake of sodium and potassium by calcite, *Chem. Geol.*, 42, 137–146

Jacob, D.E., Wirth, R., Agbaje, O.B.A. et al. (2017) Planktic foraminifera form their shells via metastable carbonate phases. *Nat Commun* 8, 1265

Keul, N., Langer, G., de Nooijer, L.J., Nehrke, G., Reichart, G.-J., Bijma, J. (2013) Incorporation of uranium in benthic foraminiferal calcite reflects seawater carbonate ion concentration. *Geochem. Geophys. Geosyst.* 14, 102–111

Langer, G., N. Gussone, G. Nehrke, U. Riebesell, A. Eisenhauer, H. Kuhnert, B. Rost, S. Trimborn, S. Thoms (2006) Coccolith strontium to calcium ratios in *Emiliana huxleyi*: the dependence on seawater strontium and calcium concentrations. *Limnol. Oceanogr.*, 51, pp. 310-320

Langer, G., Nehrke, G., Thoms, S., Stoll, H. (2009): Barium partitioning in coccoliths of *Emiliana huxleyi*. *Geochimica et Cosmochimica Acta*, 73 (10), 2899-2906 . doi: 10.1016/j.gca.2009.02.025

Langer, G., Probert, I., Nehrke, G., Ziveri, P. (2011) The morphological response of *Emiliana huxleyi* to seawater carbonate chemistry changes: an inter-strain comparison, *J. Nannoplankton Res.* 32, 27–32

Langer, G., A. Sadekov, S. Thoms, A. Mewes, G. Nehrke, M. Greaves, S. Misra, J. Bijma, and H. Elderfield (2015), Li partitioning in the benthic foraminifera *Amphistegina lessonii*, *Geochem. Geophys. Geosyst.*, 16, 4275–4279

Langer, G., Aleksey Sadekov, Silke Thoms, Nina Keul, Gernot Nehrke, Antje Mewes, Mervyn Greaves, Sambuddha Misra, Gert-Jan Reichart, Lennart Jan de Nooijer, Jelle Bijma, Henry Elderfield (2016) Sr partitioning in the benthic foraminifera *Ammonia aomoriensis* and *Amphistegina lessonii*, *Chemical Geology*, Volume 440, Pages 306-312

Lea D.W. (2014) Elemental and Isotopic Proxies of Past Ocean Temperatures. In: Holland H.D. and Turekian K.K. (eds.) *Treatise on Geochemistry*, Second Edition, vol. 8, pp. 373-397. Oxford: Elsevier

Lear, C. H., H. Elderfield, and P. A. Wilson (2003) A Cenozoic seawater Sr/Ca record from benthic foraminiferal calcite and its application in determining global weathering fluxes, *Earth Planet. Sci. Lett.*, 208, 69–84

Lorens, R. B. (1981) Sr, Cd, Mn and Co distribution coefficients in calcite as a function of calcite precipitation rate, *Geochim. Cosmochim. Acta*, 45, 553–561

Marriott, C. S., G. M. Henderson, R. Crompton, M. Staubwasser, and S. Shaw (2004a) Effect of mineralogy, salinity, and temperature on Li/Ca and Li isotope composition of calcium carbonate, *Chem. Geol.*, 212, 5–15

Marriott C. S., Henderson G. M., Belshaw N. S. and Tudhope A.W. (2004b) Temperature dependence of $\delta^7\text{Li}$, $\delta^{44}\text{Ca}$ and Li/Ca during growth of calcium carbonate. *Earth Planet. Sci. Lett.* 222(2), 615–624

Mass, Tali, Anthony J. Giuffre, Chang-Yu Sun, Cayla A. Stifler, Matthew J. Frazier, Maayan Neder, Nobumichi Tamura, Camelia V. Stan, Matthew A. Marcus, Pupa U. P. A. Gilbert (2017) *Proceedings of the National Academy of Sciences of the United States of America* vol. 114 no. 37, E7670–E7678

Mejía, L. M., Paytan, A., Eisenhauer, A., Böhm, F., Kolevica, A., Bolton, C., ... & Stoll, H. (2018). Controls over $\delta^{44}\text{Ca}/^{40}\text{Ca}$ and Sr/Ca variations in coccoliths: New perspectives from laboratory cultures and cellular models. *Earth and Planetary Science Letters*, 481, 48-60

Mewes, A., Langer, G., de Nooijer, L.J., Bijma, J., Reichart, G.-J. (2014) Effect of different seawater Mg^{2+} concentrations on calcification in two benthic foraminifers. *Marine Micropaleontology* 113, 56-64

Mewes, A., Langer, G., Thoms, S., Nehrke, G., Reichart, G.-J., de Nooijer, L.J., Bijma, J. (2015a) Impact of seawater Ca^{2+} on the calcification and calcite Mg/Ca of *Amphistegina lessonii*. *Biogeosciences* 12, 2153-2162

Mewes, A., Langer, G., Reichart, G.-J., de Nooijer, L.J., Nehrke, G., Bijma, J., (2015b) The impact of Mg contents on Sr partitioning in benthic foraminifers. *Chem. Geol.* 412, 92–98

Misra, S., M. Greaves, R. Owen, J. Kerr, A. C. Elmore, and H. Elderfield (2014), Determination of B/Ca of natural carbonates by HR-ICP-MS, *Geochem. Geophys. Geosyst.*, 15, 1617–1628, doi:10.1002/2013GC005049.

Müller, M. N., Krabbenhöft, A., Vollstaedt, H., Brandini, F. P., & Eisenhauer, A. (2018). Stable isotope fractionation of strontium in coccolithophore calcite: Influence of temperature and carbonate chemistry. *Geobiology*, 16(3), 297-306

Nehrke, G., Keul, N., Langer, G., de Nooijer, L.J., Bijma, J., Meibom, A. (2013) A new model for biomineralization and trace-element signatures of Foraminifera tests. *Biogeosciences*, 10, 6759-6767

Okumura, M., and Y. Kitano (1986) Coprecipitation of alkali metal ions with calcium carbonate, *Geochim. Cosmochim. Acta*, 50, 49–58

Russell, A. D., B. Hönisch, H. J. Spero, D. W. Lea (2004), Effects of seawater carbonate ion concentration and temperature on shell U, Mg, and Sr in cultured planktonic foraminifera, *Geochim. Cosmochim. Acta*, 68(21), 4347 – 4361

Simkiss, K., K. Wilbur, *Biomineralization* (1989) Cell Biology and Mineral Deposition, Academic Press, San Diego

Stoll, H., Langer, G., Shimizu, N., Kanamaru, K. (2012): B/Ca in coccoliths and relationship to calcification vesicle pH and dissolved inorganic carbon concentrations, *Geochimica et Cosmochimica Acta* 80, 143-157. doi: 10.1016/j.gca.2011.12.003

Tambutté E, et al. (2012) Calcein labelling and electrophysiology: Insights on coral tissue permeability and calcification. *Proc Biol Sci* 279:19–27

Taubner, I., Böhm, F., Eisenhauer, A., Garbe-Schönberg, D., Erez, J. (2012) Uptake of alkaline earth metals in Alcyonarian spicules (Octocorallia). *Geochim. Cosmochim. Acta* 84, 239–255

Taylor, Alison R., Colin Brownlee, Glen Wheeler (2017) Coccolithophore Cell Biology: Chalking Up Progress. *Annu. Rev. Mar. Sci.* 2017. 9:283–310

Urey, H.C., Lowenstam, H.A., Epstein, S., McKinney, C.R. (1951) Measurement of paleotemperatures and temperatures of the uppercretaceous of England, Denmark, and the southeastern United-States. *Geol. Soc. Am. Bull.*62, 399-416

Vidavsky N, et al. (2016) Calcium transport into the cells of the sea urchin larva in relation to spicule formation. *Proc Natl Acad Sci USA* 113:12637–12642

White, P.J. (2000) Calcium channels in higher plants, *Biochimica et Biophysica Acta (BBA)-Biomembranes*, 1465, 171–189

Yu, J., Elderfield, H., Greaves, M., and Day, J. (2007), Preferential dissolution of benthic foraminiferal calcite during laboratory reductive cleaning, *Geochem. Geophys. Geosyst.*, 8, Q06016, doi:10.1029/2006GC001571

Accepted Article

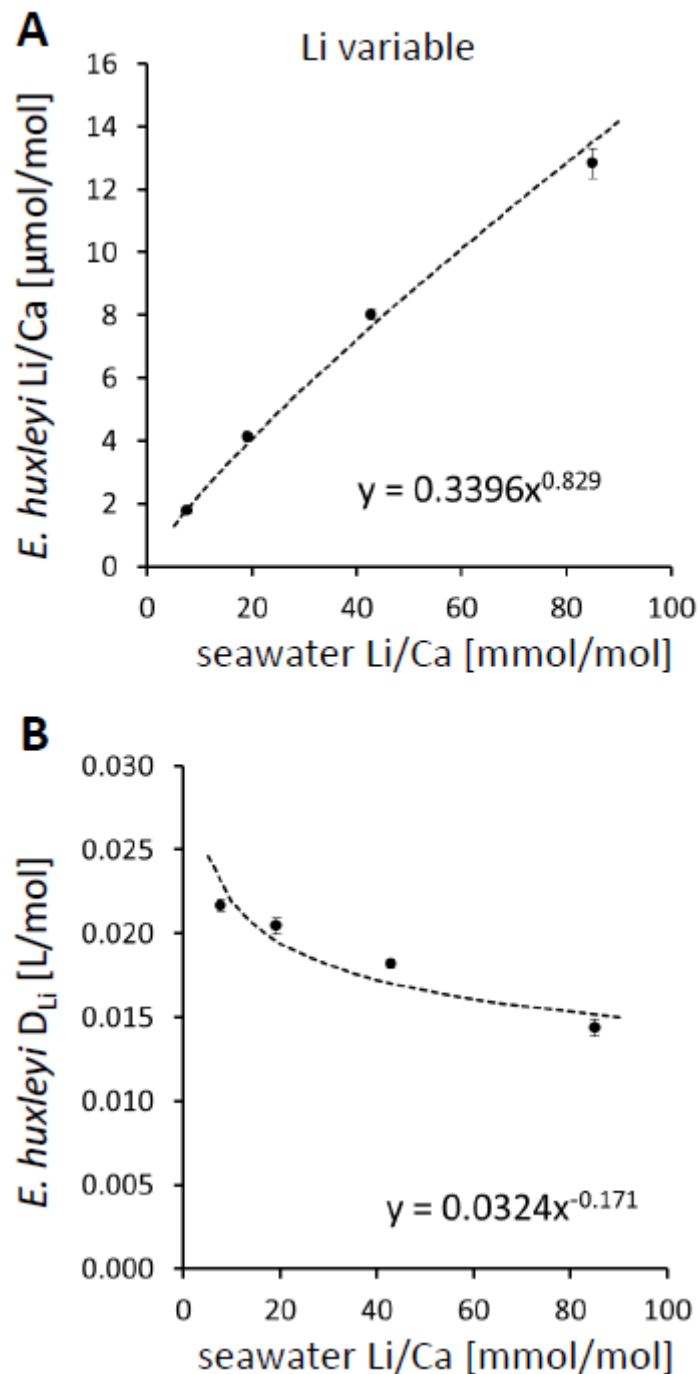


Figure 1

- A) *E. huxleyi* Li/Ca ratio [$\mu\text{mol/mol}$] versus seawater Li/Ca ratio [mmol/mol]. The seawater Li/Ca ratio was changed by changing seawater Li concentration. The dashed line was calculated using the equation shown in the plot. Error bars represent standard error.
- B) *E. huxleyi* D_{Li} [L/mol] versus seawater Li/Ca ratio [mmol/mol]. The seawater Li/Ca ratio was changed by changing seawater Li concentration. The dashed line was calculated using the equation shown in the plot. Error bars represent standard error.

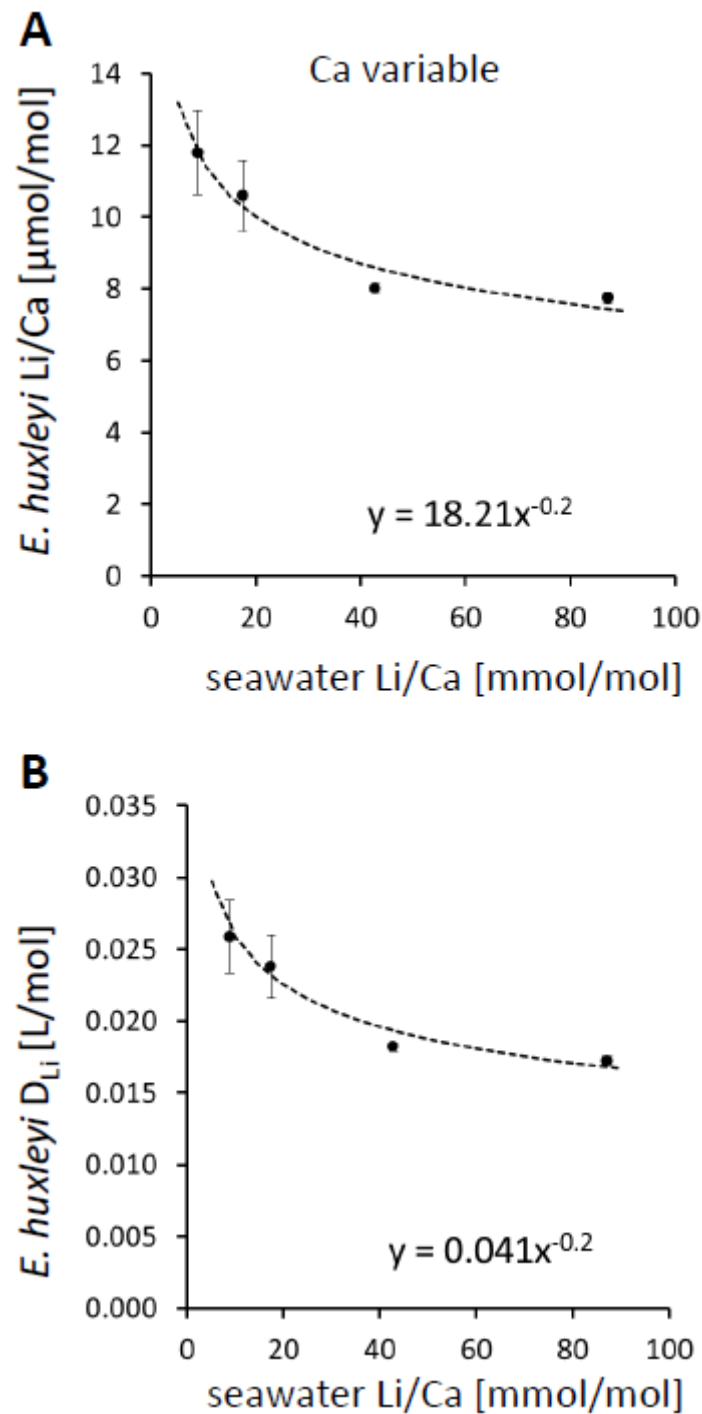


Figure 2

- A) *E. huxleyi* Li/Ca ratio [$\mu\text{mol/mol}$] versus seawater Li/Ca ratio [mmol/mol]. The seawater Li/Ca ratio was changed by changing seawater Ca concentration. The dashed line was calculated using the equation shown in the plot. Error bars represent standard error.
- B) *E. huxleyi* D_{Li} [L/mol] versus seawater Li/Ca ratio [mmol/mol]. The seawater Li/Ca ratio was changed by changing seawater Ca concentration. The dashed line was calculated using the equation shown in the plot. Error bars represent standard error.

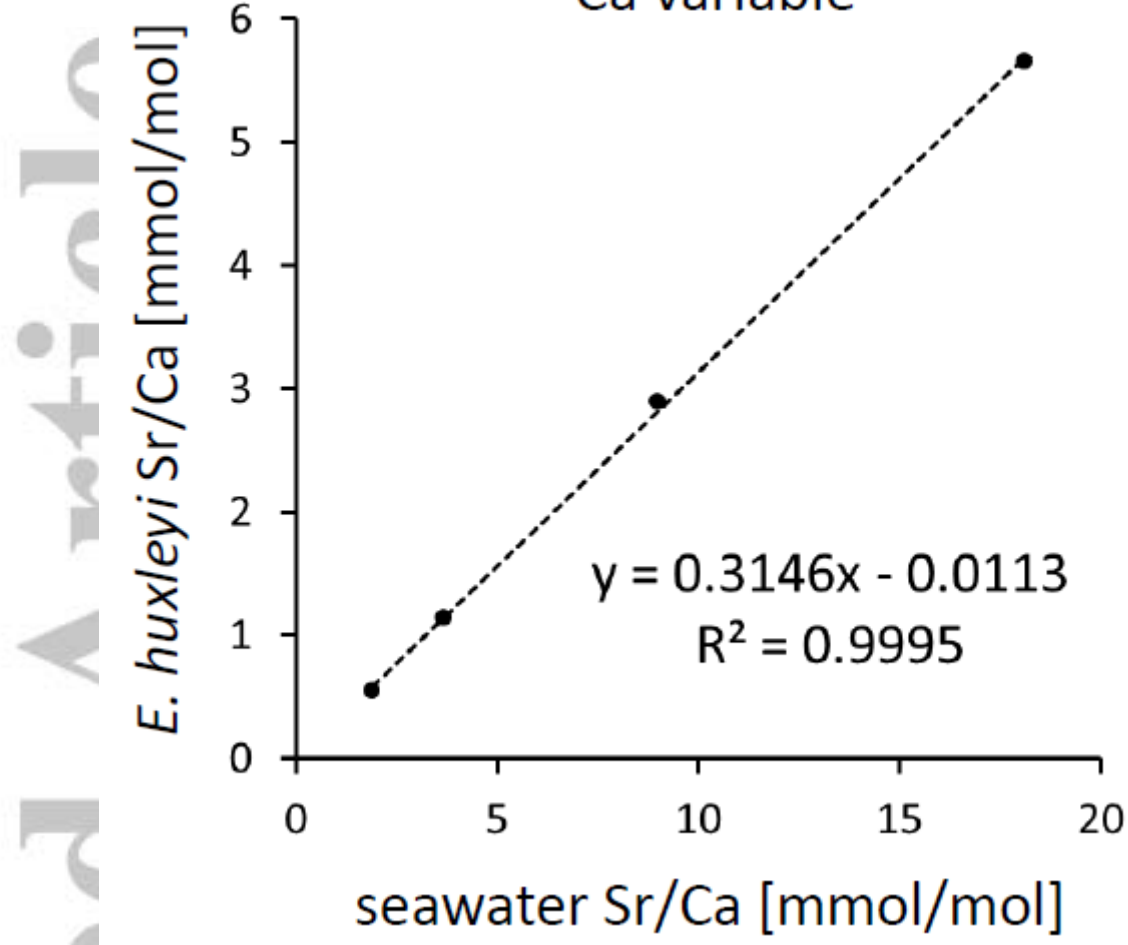


Figure 3

E. huxleyi Sr/Ca ratio [mmol/mol] versus seawater Sr/Ca ratio [mmol/mol]. The seawater Sr/Ca ratio was changed by changing seawater Ca concentration. The dashed line is the linear trend-line (equation and r^2 shown in the plot). The slope of the trend-line represents the DSr = 0.3146. Error bars represent standard error.

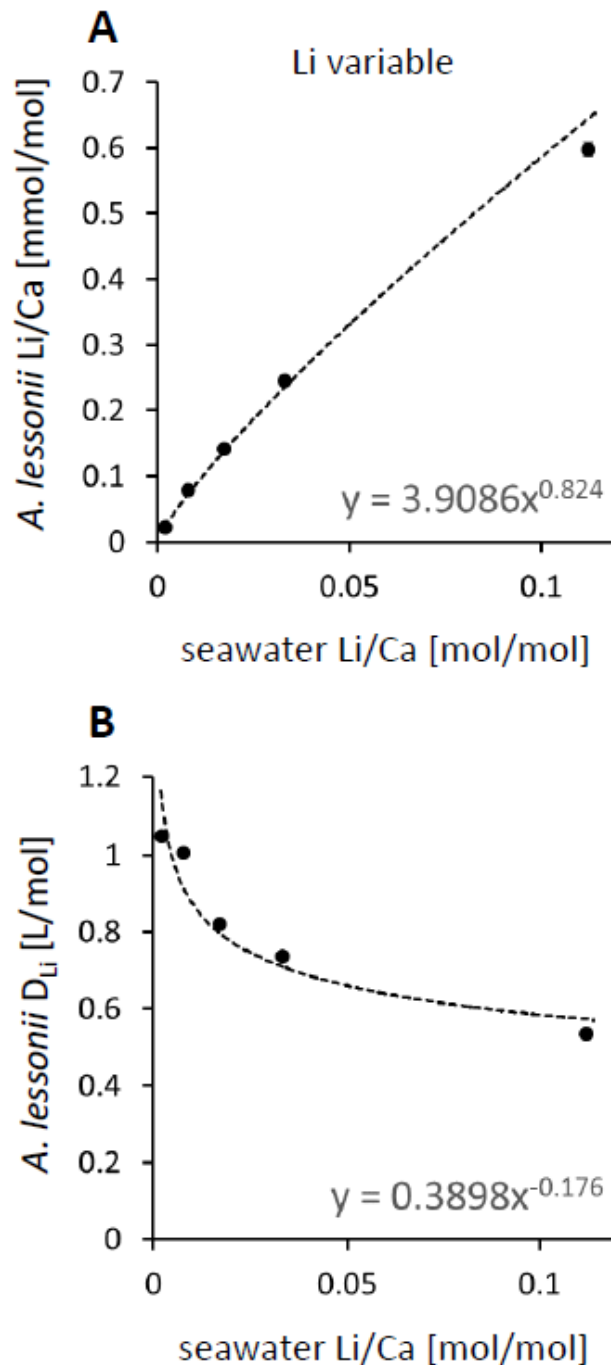


Figure 4

A) *A. lessonii* Li/Ca ratio [mmol/mol] versus seawater Li/Ca ratio [mol/mol]. The seawater Li/Ca ratio was changed by changing seawater Li concentration. The dashed line was calculated using the equation shown in the plot. Error bars represent standard error. Data from Langer et al. (2015).

B) *A. lessonii* D_{Li} [L/mol] versus seawater Li/Ca ratio [mol/mol]. The seawater Li/Ca ratio was changed by changing seawater Li concentration. The dashed line was calculated using the equation shown in the plot. Error bars represent standard error. Data from Langer et al. (2015).

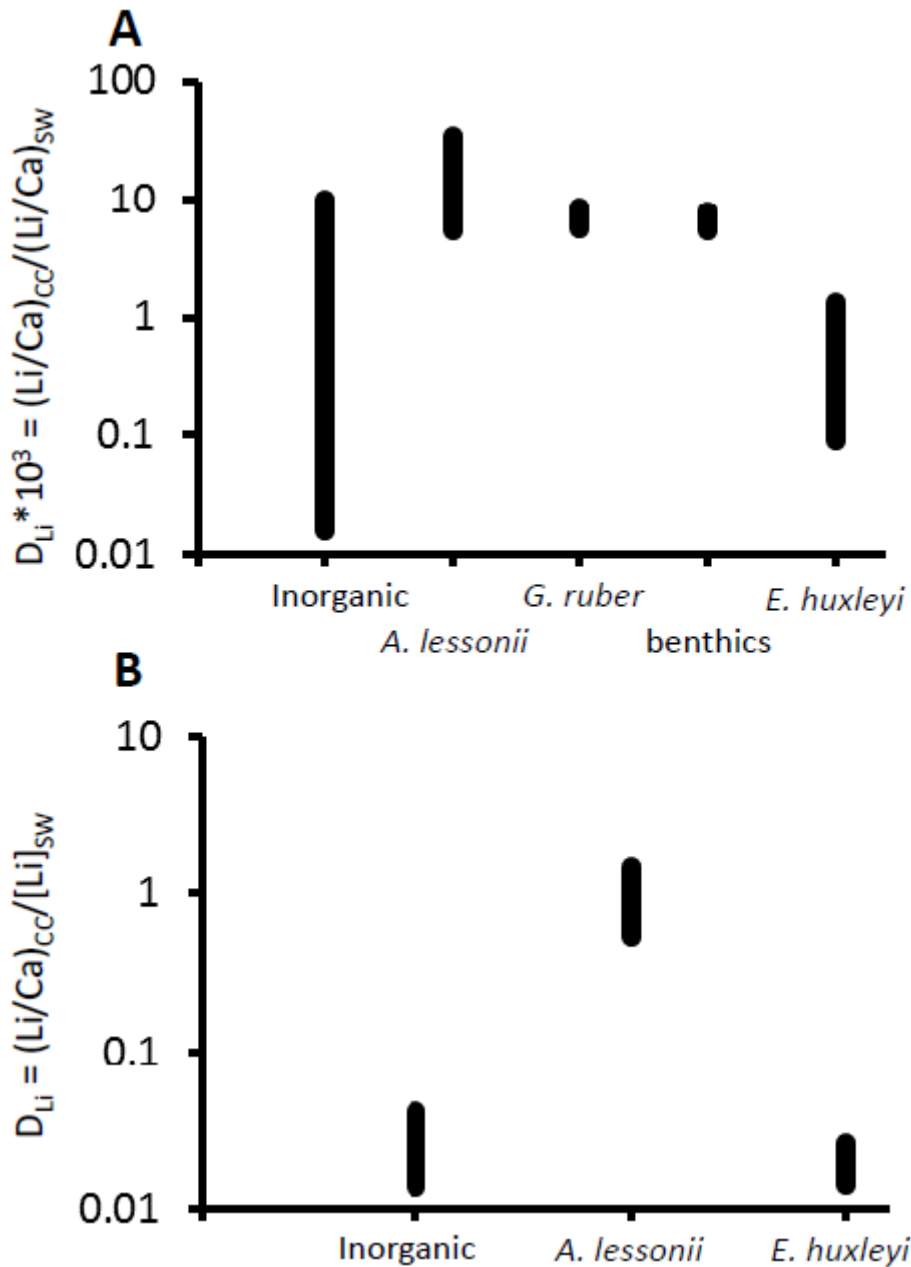


Figure 5

A) $D_{Li} * 10^3 = \frac{(Li/Ca)_{cc}}{(Li/Ca)_{sw}}$ of different calcites. Data were taken from: Inorganic: Okumura and Kitano (1986), Marriott et al. (2004a), Marriott et al. (2004b), Fuger et al. (2019). *A. lessonii*: Langer et al. (2015). *G. ruber*: Evans et al. (2018). Benthics: Marriott et al. (2004a). *E. huxleyi*: this study.

B) $D_{Li} = \frac{(Li/Ca)_{cc}}{[Li]_{sw}}$ of different calcites. Data were taken from: Inorganic: Okumura and Kitano (1986), Marriott et al. (2004b). *A. lessonii*: Langer et al. (2015). *E. huxleyi*: this study.

Table 1. Dataset derived from the experiments with *E. huxleyi*. SD = standard deviation, SE = standard error. See excel file.

seawater	seawater	seawater	seawater	coccoliths	coccoliths	coccoliths	coccoliths	coccoliths	coccoliths	coccoliths	coccoliths	coccoliths	coccoliths	coccoliths	coccoliths	coccoliths
Li/Ca	Sr/Ca	[Ca]	[Li]	Li/Ca	Li/Ca	Li/Ca	DLi	DLi	DLi	Sr/Ca	Sr/Ca	Sr/Ca	DSr	DSr	DSr	
mmol/mol	mmol/mol	mM	mM	$\mu\text{mol/mol}$	$\mu\text{mol/mol}$	$\mu\text{mol/mol}$	L/mol	L/mol	L/mol	mmol/mol	mmol/mol	mmol/mol	mol/mol	mol/mol	mol/mol	
				average	SD	SE	average	SD	SE	average	SD	SE	average	SD	SE	
Ca variable																
8.8778	1.8878	51.2997	0.4554	11.7804	2.3358	1.1679	0.0259	0.0051	0.0026	0.5470	0.0027	0.0013	0.2898	0.0014	0.0007	
17.4384	3.6936	25.5100	0.4449	10.5786	1.9596	0.9798	0.0238	0.0044	0.0022	1.1411	0.0042	0.0021	0.3089	0.0011	0.0006	
42.8061	8.9819	10.3055	0.4411	8.0220	0.2643	0.1321	0.0182	0.0006	0.0003	2.8930	0.0314	0.0157	0.3221	0.0035	0.0017	
87.1270	18.1223	5.1587	0.4495	7.7428	0.3006	0.1503	0.0172	0.0007	0.0003	5.6569	0.0643	0.0321	0.3121	0.0035	0.0018	
Li variable																
85.0525	8.6735	10.4984	0.8929	12.8377	0.9423	0.4712	0.0144	0.0011	0.0005	2.8073	0.0102	0.0059	0.3237	0.0012	0.0007	
42.8061	8.9819	10.3055	0.4411	8.0220	0.2643	0.1321	0.0182	0.0006	0.0003	2.8930	0.0314	0.0157	0.3221	0.0035	0.0017	
19.1934	8.6053	10.5258	0.2020	4.1315	0.2009	0.1005	0.0205	0.0010	0.0005	2.8021	0.0102	0.0051	0.3256	0.0012	0.0006	
7.7179	8.6129	10.5816	0.0817	1.7705	0.0622	0.0311	0.0217	0.0008	0.0004	2.7468	0.0089	0.0063	0.3189	0.0010	0.0007	